CORROSION SCIENCE AND TECHNOLOGY, Vol.31, No.4(2002), pp.320~326

Effect of the Microstructure of Inconel 600 HTMA on Susceptibility to Stress Corrosion Cracking on the Simulated Nuclear Power Plant Operating Conditions

Joung Soo Kim, Jung Ho Han, Hong Pyo Kim, Yun Soo Lim, Deok Hyun Lee, Seong Sik Hwang, and Do Haeng Hur

Korea Atomic Energy Research Institute
P.O.Box 105, Yuseong, Daejeon, Korea

It has been known that Inconel 600 material having been used for long time as steam generator tubing is susceptible to various localized corrosion, such as pitting, stress corrosion cracking, fretting, denting, etc., in the nuclear power plant operating conditions. Of the localized corrosion, stress corrosion cracking (SCC), nowadays, is a dominant defect mechanism occurring in steam generator tubing of domestic as well as world wide nuclear plants. The susceptibility of Inconel 600 material to SCC has been reported to be very sensitive to its microstructure. In this study, the susceptibility of archive Inconel 600 high temperature mill annealed(HTMA) tubing having been used in steam generators on the operating nuclear power plants in Korea was investigated by changing its microstructure in order to see the degree of the integrity of the tubing. According to the results, the susceptibility of the material to primary and secondary water SCC(PWSCC and IGSCC) is very sensitive to the microstructure of even the as-received tubing material and also to the microstructure modified using additional heat treatments under a simulated nuclear power plant operating conditions. It was confirmed that the resistance of the Inconel 600 HTMA material to SCC can be improved much by modifying its microstructure using proper heat treatments.

Keywords : *steam generator, alloy 600, stress corrosion cracking, pressurized water reactor, primary water stress corrosion cracking, high temperature mill annealing*

1. Introduction

Alloy 600 has been observed to be susceptible to primary water SCC (PWSCC). Therefore many researches have been undertaken to make the cracking mechanism clear, but it is still under the debate. The chemical element compositions and carbide morphologies along grain boundaries of the material are considered to be a plausible solution to explain the crack mechanism.

Intergranular stress corrosion cracking (IGSCC or ODSCC) of Alloy 600 has also occurred at crevices between tubing and tubesheet, tubing and tube support plate or tubing and sludge piled on the top of tubesheet because impurities segregated into the crevices due to higher temperature in the crevices than that of the secondary coolant in pressurized water reactors (PWRs). pH in the crevices can be acidic or alkaline depending on the impurities segregated in the crevices.[1),2)] Even though recent works suggest that crevice solution be in mid-range pH or light alkaline based on the analysis of corrosion products on steam generator tubing,[3)] there is still possibility that the crevice can be acidic or alkaline in steam generator depending on the operating conditions of plants.

This article aims to know the effect of a thermal treatment on high temperature mill annealed (HTMA) Alloy 600 tubing, which is one of archive steam generator tubing in Korean nuclear power plants.

2. Experimental

2.1 Microstructures

Microstructures, cross-sectional areas showing crack paths, and SCC fracture surfaces of the test specimens were examined using optical microscope(OM), scanning electron microscope(SEM), and transmission electron microscope(TEM).

2.2 Primary water SCC

Materials used in PWSCC test were Alloy 600HTMA, Alloy 600TT, Alloy 600 Serrated (SR). Alloy 600 TT and

Table 1. Alloy designation and chemical compositions of steam generator tubes

Designation	Ni	Cr	Fe	C	S	P	B	N	Si	Cu	Al	Ti
Alloy 600 HTMA	76.11	15.29	7.57	0.026	0.001	0.008	0.004	0.004	0.15	0.015	0.23	0.32
Alloy 600 LTMA	74.66	15.21	9.16	0.022	0.001	0.003			0.2	0.01	0.24	0.29
Alloy 690 TT	58.9	29.57	10.54	0.02	0.001	0.009	0.004	0.017	0.22	0.01	0.019	0.26

Table 2. Mechanical properties of steam generator tubing.

Alloy	Yield strength (MPa)	Tensile strength (MPa)	Elongation (%)	ASTM Grain size
Alloy 600 HTMA	258	675	43	6
Alloy 600 LTMA	310	679	44	
Alloy 690 TT	330	730	44	

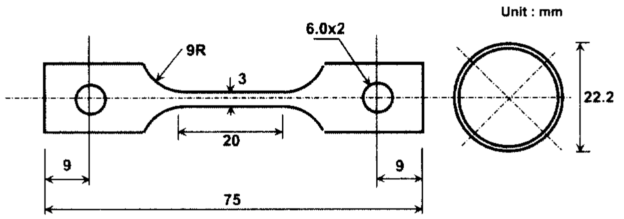

Fig. 1. The shape and dimensions of the CERT specimen used in this study.

Alloy 600 SR were prepared by thermal treating the as-received Alloy 600 HTMA at 700°C for 16 hours and 715 °C for 15 hours, respectively. Alloy designations and their chemical compositions are shown in Table 1. The mechanical properties of the alloys are summarized in Table 2.

PWSCC susceptibility was characterized using a constant extension rate tester(CERT). The tensile specimen was prepared as shown in Fig. 1. The test vessel made of 316 stainless steel is equipped with pressure balanced pull rod and water supplying loop system, which can simulate the primary coolant conditions of PWR. The solution was consisted of 2.0 ppm Li and 1200 ppm of Boron, and a dissolved hydrogen content of 35 cc/kg H_2O. Four tensile specimens insulated electrically with zirconia(ZrO_2) were tested at the same time, and time to failure, maximum load and elongation were measured from the load variation during the test and the final elongation after the test.

2.3 Secondary water stress corrosion cracking

The materials were the nuclear grade Alloy 600 HTMA as used in PWSCC, Alloy 600 LTMA(low temperature mill annealed) and Alloy 690 TT(thermally treated), the chemical compositions of which are shown in Table 1. Alloy 600 SN(sensitized) and Alloy 600 TT were prepared by heat treating the as-received Alloy 600 HTMA at 600°C for 24 hours and 715°C for 15 hours, respectively. Some of the tubes were elongated by 20% to increase their yield strength and thereby apply higher stress at the apex of C-ring specimens. Maximum tensile stress was about 340 MPa at the apex of the C-ring specimen for the as-received Alloy 600 HTMA while that is about 565 MPa for the 20 % elongated Alloy 600 HTMA.

All test solutions was prepared by adding reagent grade chemicals to demineralized water. A modified Huey test was carried out in boiling 25 % HNO_3 for 48 hours. SCC test solutions were 0.1 M $NaHSO_4$, 0.1 M Na_2SO_4, and 1 %, 10 % and 40 % NaOH solutions. The solutions were deoxygenated by purging nitrogen gas into the autoclave and then venting the gas through water. SCC tests were performed using C-ring specimens at corrosion potential in the 0.1 M $NaHSO_4$, 0.1 M Na_2SO_4 and at 200 mV above the corrosion potential in the 1 %, 10 % and 40 % NaOH solutions. Reference and counter electrodes were an external Ag/AgCl electrode and Pt wire, respectively. The stress at the apex of the C-ring specimen was measured to range from about 300 MPa to about 565 MPa. SCC test matrix is shown in Table 3.

Table 3. IGSCC test matrix.

SCC test matrix				
Solution : 0.1M$NaHSO_4$, 0.1M Na_2SO_4, 1% NaOH, 10% NaOH, 40% NaOH				
Alloy designation/ Cold Work (%)	Stress (MPa)			
	300	340	450	565
Alloy 600 HTMA/0		o		
Alloy 600 HTMA/20				o
Alloy 600 SN/0	o	o		
Alloy 600 SN/20	o	o	o	o
Alloy 600 TT/0		o		
Alloy 600 TT/20		o	o	o
Alloy 600 LTMA/0	o	o		
Alloy 600 LTMA/20	o	o	o	o

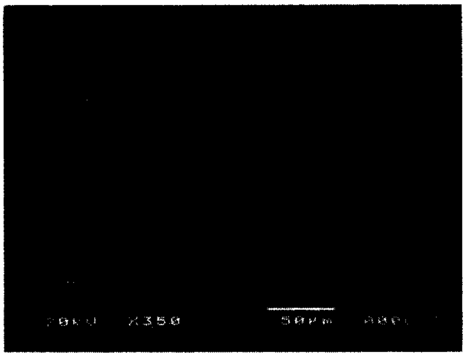

(a)

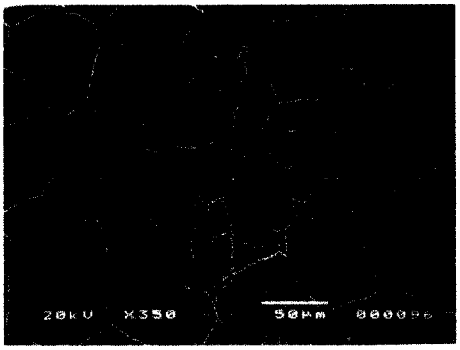

(b)

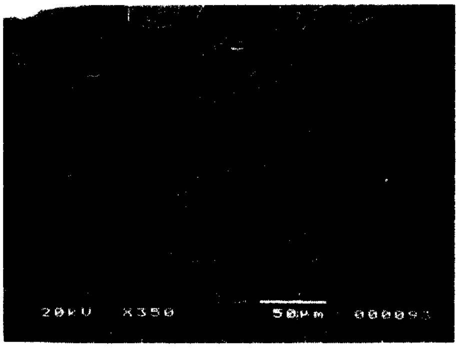

(c)

Fig. 2. Optical microstructures of (a) Alloy 600 HTMA, (b) Alloy 600 serrated, and (c) Alloy 600 TT

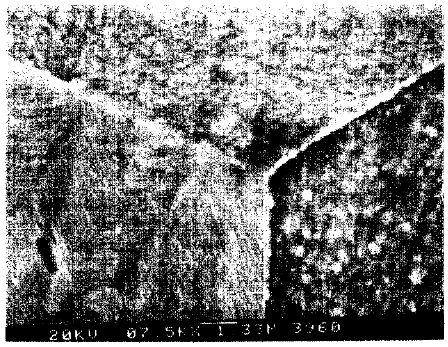

(a)

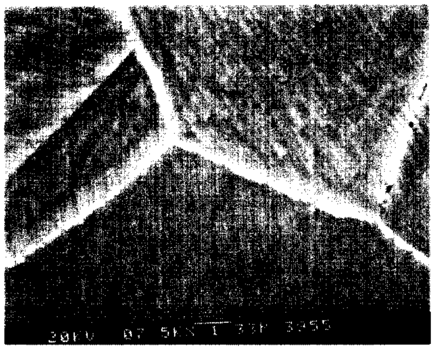

(b)

(c)

Fig. 3. Intergranular carbide distribution in (a) Alloy 600 HTMA, (b) Alloy 600 SN, and Alloy 600 TT observed with SEM after etching in bromine solution.

3. Results and discussion

3.1 Microstructures

Optical microstructures of high temperature mill annealed(HTMA), serrated(SR), thermally treated (TT), and SEM microstructures of Alloy 600 HTMA, sensitized(SN) Alloy 600s, and Alloy 600 TT are shown in Fig. 2 and 3, respectively. High temperature mill annealed Alloy 600 shows intergranular carbide distribution varying even in a grain boundary and also varying from boundary to boundary.(Fig. 2 and 3)) Intergranular carbide distributions in Alloy 600 SN and Alloy 600 TT are semi-continuous and almost uniform within a boundary and more homogenous from boundary to boundary compared to HT 600.(Fig. 2 and 3) However, serrated Alloy 600 shows zig-zag grain boundary morphology and the distribution and size of Cr carbide precipitated along grain boundaries are discontinuous and relatively large compared to other specimens.(Fig. 2)

The Cr concentrations were measured for the three differently heat treated specimens using TEM attaching an energy dispersion X-ray spectroscope (EDX). The

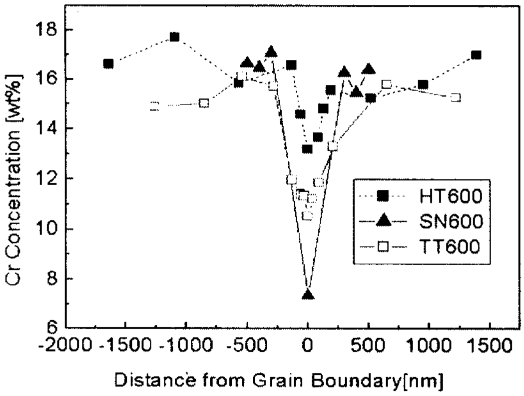

Fig. 4. Cr concentration profiles across the grain boundaries of the Alloy 600s

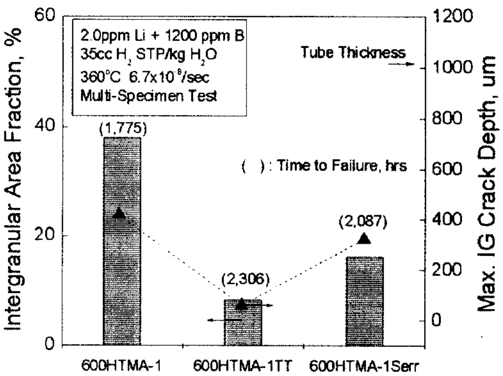

Fig. 5. Susceptibility to PWSCC of the Alloy 600s

minimum Cr concentrations of the three specimens were about 7 wt%, 13 wt%, and 10.5 wt% for Alloy 600 SN, HTMA, and TT, respectively, as shown in Fig. 4

3.2 Primary water SCC

SCC tests were performed with Alloy 600 HTMA, Alloy 600 SR, and Alloy 600 TT in a simulated primary cooling solution containing 2.0 ppm Li, 1200 ppm B, and 35cc H_2 STP/kg H_2O at 360°C. The extension rate in the constant extension rate test(CERT) was 6.7×10^{-8}/sec.. According to the test results, SCC resistance in the primary water increased as a sequence of Alloy 600 HTMA, Alloy 600 SR, and Alloy 600TT. The crack length was longer in the specimen on which short cracking time was short.

For better quantification data, maximum and average crack propagation rate were presented in Fig. 5. The calculated velocities were obtained by the formula as below.

Maximum crack propagation=
maximum crack length/failure time,
Average crack propagation=
specimen thickness*IG fracture/(2* failure time)

SCC resistance of the materials is reported to be related with the carbide structure of the specimens.[4)] Alloy 600 HTMA additionally thermally treated at 700 C for 16 hours to see the effect of thermal treatment showed a high SCC resistance of 5 times larger than the as-received one. As shown in Fig. 5 serration heat treatment also gives better effect on the increase of SCC resistance. The serrated specimen showed increased time to failure and decreased intergranular area fraction. This result means that SCC resistance of Alloy 600 can be increased by the heat treatment to develop intergranular carbides along the grain boundary or a formation of serrated grain boundary.

3.3 Secondary water SCC

3.3.1 SCC in sulfate.

M $NaHSO_4$. All of the Alloy 600 HTMA and SN were completely through wall cracked and Alloy 600 TT was almost through wall cracked in 34 days tested in 0.1 M $NaHSO_4$ for the C-ring specimen with an initial stress of 565 MPa. On the other hand, all Alloy 600 specimens were slightly cracked in 34 days tested in 0.1 M $NaHSO_4$ for a C-ring specimen with an initial stress of 340 MPa as shown in Fig. 6. However, Alloy 690 TT was not cracked in the same solution even at an initial stress of 565 MPa. Relative SCC resistance of the tube materials was determined by destructive examination after 34 days immersion tests. SCC resistance in 0.1 M $NaHSO_4$ increased in order of Alloy 600 SN, Alloy 600 HTMA, Alloy 600 TT, and Alloy 690 TT. Neither intergranular carbide distribution nor Cr depletion alone could explain the SCC resistance of the heat- treated Alloy 600. Alloy 600 SN was most amenable to SCC possibly due to heavy chromium depletion around grain boundaries even though Alloy 600 SN has almost continuous intergranular carbide, while Alloy 600 HTMA having discrete intergranular carbide distribution along grain boundaries was more resistant to SCC than Alloy 600 SN. Higher resistance of Alloy 600 HTMA compared to Alloy 600 SN suggests that the harmful effects of chromium depletion around grain boundaries overwhelm the beneficial effect of the intergranular carbide precipitated along grain boundaries. However, higher resistance of Alloy 600 TT compared to Alloy 600 HTMA suggests that the role of intergranuar carbide becomes dominant over the critical chromium concentration at grain boundaries. SCC growth rates of the specimens in 0.1 M $NaHSO_4$ are shown in Table 4.

0.1M Na_2SO_4. No SCC was observed on the C-ring specimens having an initial stress at the apex in the range from 300 MPa to 565 MPa and exposed to the 0.1 M $NaSO_4$ solution at 360°C for 34 days.

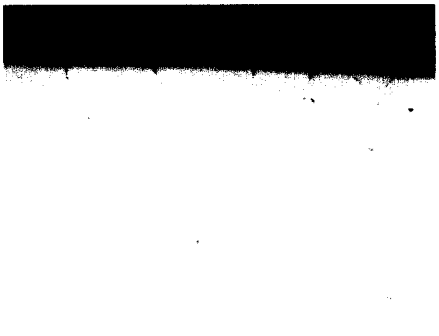

Alloy 600 HTMA

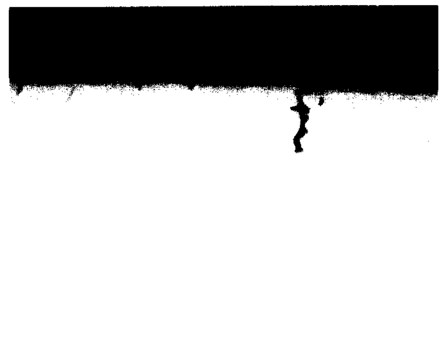

Alloy 600 SN

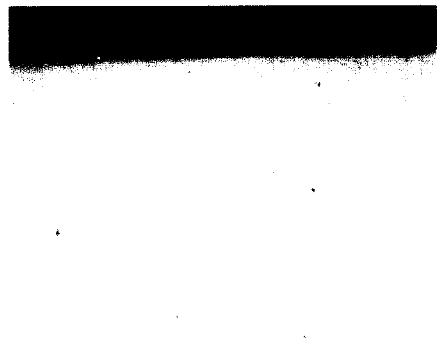

Alloy 600 TT

Fig. 6. Cross sectional area of C-ring specimen of Alloy 600 at an initial stress of 340 MPa exposed to 0.1 M $NaHSO_4$ 34 days.

Table 4. Measured SCC rates of Alloy 600s.

Alloy 600	SCC rate ($\times 10^{-9}$m/sec)		
	0.1M $NaHSO_4$	10% NaOH	40% NaOH
Alloy 600 HTMA	0.018	1.7	5.4
Alloy 600 SN	0.031	0.13	3.1
Alloy 600 TT	0.003	0.08	1.5

3.3.2 SCC in caustic.

SCC growth rates of Alloy 600 LTMA(low temperature mill annealed), Alloy 600 HTMA and Alloy 600 TT with an initial stress of 565 MPa tested in 10 % NaOH at 315°C are summarized in Table 4. Alloy 600 LTMA was most susceptible to SCC among the tube materials. However, Alloy 690 TT exposed to 10 % NaOH for 15 days showed no SCC. Four Alloy 600 HTMA materials having been fabricated by three different vendors presented nearly same susceptibility to SCC in the 10% NaOH solution and under high stress(565 Mpa) imposed to the specimens.

Features of the cross sectional area of the C-ring specimens after exposure to 10 % NaOH for 9 days and 40 % NaOH for 2 days are shown in Fig. 7 and 8 respectively. The C-ring specimens were bent to open the cracks after SCC test and then the cross sectional areas of the C-ring specimens were examined with an optical microscope. The SCC resistance of Alloy 600s in 10 % and 40 % NaOH solutions increased in order of Alloy HTMA, Alloy 600 SN, and Alloy 600 TT. However, no SCC was observed after 36 day test in 1% NaOH at 315°C, where the stress at the apex of the C-ring specimen was ranging from 300 MPa to 565 MPa.

All Alloy 600 HTMA tube materials tested in 10 % NaOH showed similar SCC resistance probably due to similar microstructure and mechanical properties as shown in Table 5(HP Kim's paper Table 3) or due to too aggressive environment which can not differentiate the distinction among them. These results are consistent with finding by Jacko that subtle differences were observed to occur depending on heats tested in 1 % NaOH at 316°C and 343°C, and in 10 % NaOH at 288°C, 302°C and 332 oC for a mill annealed Alloy 600 or thermally treated Alloy 600.[5)]

According to the test results in 10% NaOH and 40% NaOH, Alloy 600 LTMA showed the least resistance to SCC, while Alloy 600 TT was the most resistance to SCC. This suggests that chromium depletion is not detrimental to SCC in alkaline solution, and the role of intergranular carbide distribution becomes more prominent in SCC in alkaline solution than in acidic solution(0.1 M $NaHSO_4$). Higher SCC resistance of Alloy 600 TT compared to Alloy 600 SN seems to be primarily due to the thickness and length of intergranular carbide in Alloy 600 TT and secondarily due to healing chromium depletion around grain boundaries.

In order to see crack initiation, the C-ring specimens were withdrawn every 7 days and examined with optical microscope. SCC crack was not observed until 34 days exposure to the 0.1 M $NaHSO_4$ solution due to thick oxide film formed on the specimen.

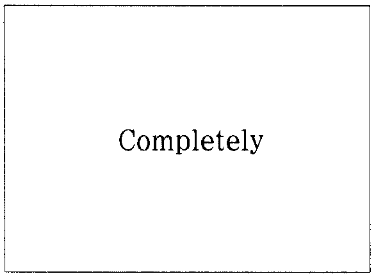

Alloy 600 HTMA

Alloy 600 SN

Alloy 600 TT

Fig. 7. Cross sectional area of C-ring specimen of Alloy 600 at an initial stress of 565 MPa exposed to 10 % NaOH for 9 days.

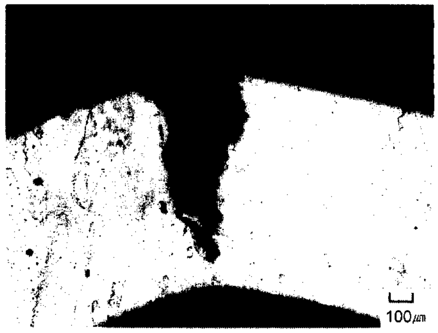

Alloy 600 HTMA

Alloy 600 SN

Alloy 600 TT

Fig. 8. Cross sectional area of C-ring specimen of Alloy 600 at an initial stress of 340 MPa exposed to 40 % NaOH for 2 days.

Even though microstructural features did not vary independently in this work because they changed simultaneously upon heat treatment, it might be surmised from these results that microstructural features that have of prime importance on SCC in alkaline solution are thickness and length of intergranular carbides. SCC resistance of alloy 600 might be given in terms of microstructure as F(line coverage of intergranular carbide). G(thickness of intergranular carbide).H(chromium depletion at grain boundary) where relative contribution of each function to SCC depends on the test environment.

According to the results obtained from this study, the susceptibility of the material to primary and secondary water SCC(PWSCC and IGSCC) is very sensitive to the microstructure of even the as-received tubing material and also to the microstructure modified using additional heat treatments under a simulated nuclear power plant operating conditions. It would be concluded that the resistance of the Inconel 600 HTMA tube material to SCC can be improved much by modifying its microstructure using proper heat or thermal treatments.

4. Conclusions

1) High temperature mill annealed Alloy 600 observed to be more susceptible to PWSCC than Alloy 600 HTMA thermally treated at 700 C for 16 hours.

2) Sensitized Alloy 600 was most susceptible to SCC in acidic solution probably due to the presence of Cr depletion zone along the grain boundaries, while Alloy 600 TT was most resistant to SCC due to the presence of semi-continuous intergranular carbides and healing of Cr depletion zone along the grain boundaries.

3) The SCC resistance of Alloy 600 in alkaline solution increased in order of Alloy 600 HTMA, Alloy 600 SN, and Alloy 600 TT.

4) Alloy 690 TT showed no crack tested in all conditions used in this study, which means that Alloy 690 TT is high resistant to both PWSCC and IGSCC.

5) The resistance of the Inconel 600 HTMA tube material to SCC can be improved much by modifying its microstructure using proper heat or thermal treatments.

Acknowledgement

This work was carried out as a part of the steam generator materials project under the nuclear R&D program sponsored by MOST in Korea.

References

1. J. P. N. Paine, S. A. Hobart, and S. G. Sawochka, "Predicting Steam Generator Crevice Chemistry", 5th International Symposium on Environmental Degradation of Materials in Nuclear Power Systems-Water Reactors, (Monterey, CA), p.739 (1991).
2. C. Goffin, J. Jadot and L. Duvivier, "Simulation of the Concentration Process in a Secondary Side Steam Generator Crevice", (Fontevraud IV, France), p.441 (1998).
3. P. M. Scott and P.Combrade, "On the Mechanisms of Secondary Side PWR Steam Generator Tube Cracking", 9th International Symposium on Environmental Degradation of Materials in Nuclear Power Systems-Water Reactors (Amelia Island, FL), p.65 (1997).
4. S.M. Bruemmer, corrosion 87, paper number 88, NACE, (1987).
5. R. J. Jacko, "Corrosion Evaluation of Thermally Treated Alloy 600 Tubing in Primary and Faulted Secondary Water Environments", EPRI NP-6721-ISD, (1990).